Available online at www.sciencedirect.com
SCIENCE DIRECT®
Journal of Magnetism and Magnetic Materials 279 (2004) 210–217
Journal of magnetism and magnetic materials
www.elsevier.com/locate/jmmm

Preparation and characterization of (3-aminopropyl) triethoxysilane-coated magnetite nanoparticles

M. Yamaura[a,*], R.L. Camilo[a], L.C. Sampaio[b], M.A. Macêdo[c], M. Nakamura[d], H.E. Toma[d]

[a] *Instituto de Pesquisas Energéticas e Nucleares, Centro de Quimica e Meio Ambiente, Av. Prof. Lineu Prestes, 2242, São Paulo – SP CEP 05508-000, Brazil*
[b] *Centro Brasileiro de Pesquisas Físicas, Rio de Janeiro – RJ CEP 22290-180, Brazil*
[c] *Universidade Federal de Sergipe, São Cristovão – SE CEP 49100-000, Brazil*
[d] *Instituto de Química da Universidade de São Paulo, São Paulo – SP C.P. 26077, Brazil*

Received 10 December 2003; received in revised form 22 January 2004

Abstract

Magnetite nanoparticles coated with (3-aminopropyl)triethoxysilane, $NH_2(CH_2)_3Si(OC_2H_5)_3$, were prepared by silanization reaction and characterized by X-ray diffractometry, transmission electron microscopy, atomic force microscopy, Fourier transform infrared spectroscopy and magnetization measurements. Both uncoated and organosilane-coated magnetite exhibited superparamagnetic behavior and strong magnetization at room temperature. Basic groups anchored on the external surface of the coated magnetite were observed. The superparamagnetic particles of coated magnetite are able to bind to biological molecules, drugs and metals and in this way remove them from medium by magnetic separation procedures.

PACS: 75.50.K; 81.05.Y

Keywords: Nanoparticles; Superparamagnetism; APTES; Coprecipitation; Silanization reaction

1. Introduction

Modified magnetic materials are nowadays well-known and have been investigated intensively due to their potential applications in many areas, such as biology, medicine and the environment. These applications include enzyme and protein separations, RNA and DNA purifications [1–3], magnetic resonance imaging (MRI) techniques for cancer diagnosis, and cancer therapy such as magnetically controllled drug carriers and hyperthermia [4–8]. Another important example is removal of toxic elements from industrial wastes [9–12]. Modified magnetic materials are composed of an iron oxide core coated with organic or inorganic molecules, which form a chemical bond with the core surface. The iron oxide core is obtained as a fine powder containing nanometer-sized particles and presents superparamagnetic behavior. Functional groups tailored for specific

*Corresponding author. Tel.: +55-11-38169334; fax: +55-11-38169325.
E-mail address: myamaura@ipen.br (M. Yamaura).

0304-8853/$ - see front matter © 2004 Elsevier B.V. All rights reserved.
doi:10.1016/j.jmmm.2004.01.094

tasks are anchored as an organic molecule shell around of the core. These particles are capable of forming stable aqueous suspensions and may be easily redispersed after agglomeration in the presence of a magnetic field.

In the present study, we report the preparation of superparamagnetic magnetite particles that were coated with (3-aminopropyl)triethoxysilane, $NH_2(CH_2)_3Si(OC_2H_5)_3$. This organosilane can bind to a metal oxide by adsorption or covalent bonding, and through the active amino group in its structure is able to combine with biomolecules, drugs and metals. This paper provides a detailed study of the preparation and characterization of the silanized magnetite nanoparticles.

2. Experimental

2.1. Preparation of magnetic nanoparticles and coating procedure

Magnetite particles were prepared by the coprecipitation method, by adding a 5 mol/l NaOH solution into a mixed solution of 0.25 mol/l ferrous chloride and 0.5 mol/l ferric chloride (molar ratio 1:2) until obtaining pH 11 at room temperature. The slurry was washed repeatedly with distilled water. Then particles were magnetically separated from the supernatant and redispersed in aqueous solution at least three times, until obtaining pH 7. After that, the surface of these particles was coated with (3-aminopropyl)triethoxysilane (APTES) by a silanization reaction in order to obtain modified magnetic particles. The procedure consisted of heating the magnetite suspension with glycerol and 40 ml of a 10% water solution of APTES (pH 4.0, adjusted with glacial acetic acid) on a water bath for 3 h. In the sequence, after magnetic separation, the silanized magnetite particles were thoroughly washed with distilled water and dried, yielding a fine powder.

2.2. Characterization

The crystalline phases were identified by means of X-ray diffraction measurements using Cu Kα radiation ($\lambda = 1.5406$ Å) at 40 kV/40 mA on Rigaku RINT 2000/PC diffractometer, in the Bragg–Bretano geometry in the 2θ range of 10–90°, in steps of 0.02°, and with a counting time of 10 s per step.

The particle size and morphology of the modified particles were obtained using a Jeol-2000EX transmission electron microscope (TEM). Atomic force microscope (AFM) images of the APTES-magnetite particles were obtained using a PicoSPM equipment from Molecular Imaging, employing MAC® Mode with Type II MACLevers, ($k \sim 2.8$ N/m; $f \sim 60$ kHz), at a typical amplitude setpoint of 6.56 V under ambient conditions. The samples were prepared by depositing microvolumes of the APTES-magnetic particle solution onto high-grade mica and allowing to dry in a laminar flow clean chamber at room temperature. Sample preparation was also carried out in a similar way, but applying a strong magnetic field (0.3 T) parallel to the flat mica surface, along with the drying process.

Fourier transform infrared (FTIR) spectrum from the KBr pellet with APTES-magnetite particles was recorded on FTIR spectrometer Nicolet, Nesus 670.

Magnetization measurements were obtained at room temperature in magnetic fields up to 10 kOe using a vibrating sample magnetometer (Princeton Applied Research, model 530).

3. Results and discussion

3.1. Preparation of magnetic nanoparticles

The coprecipitation process to obtain magnetite particles, Fe_3O_4, through reaction (1) was carried out in an aqueous medium. Magnetite nanoparticles are very sensitive to oxygen, and in the presence of air some might undergo oxidation to $Fe(OH)_3$ as shown in reaction (2) [13], or to maghemite (γ-Fe_2O_3) phase according to reaction (3). The formation of hematite (α-Fe_2O_3) is more difficult than that of the maghemite phase, occurring only under thermal dehydration conditions. Furthermore, small amounts of O_2 in water could easily oxidize the Fe^{2+} species to Fe^{3+}

through reaction (4) becoming a favorable environment for the production of $Fe(OH)_3$ or γ-Fe_2O_3 through reactions (5) and (6), respectively. The formation of these iron species is strongly dependent of the reaction kinetics and reaction temperature. Depending on pH of the aqueous solution containing Fe^{3+} ions, it is still possible to form goethite, α-FeOOH, through reaction (7) or by hydrolysis through reaction (8). The final product obtained from the coprecipitation of the present work was dense, black and magnetic. Considering those physical aspects, the final product can be identified as magnetite particles.

$$Fe^{2+} + 2Fe^{3+} + 8OH^- \rightarrow Fe_3O_4 + 4H_2O, \quad (1)$$

$$Fe_3O_4 + \tfrac{1}{4}O_2 + 4.5H_2O \rightarrow 3Fe(OH)_3, \quad (2)$$

$$2Fe_3O_4 + \tfrac{1}{2}O_2 \rightarrow 3Fe_2O_3, \quad (3)$$

$$Fe^{2+} + \tfrac{1}{2}H_2O + \tfrac{1}{4}O_2 \rightarrow Fe^{3+} + OH^-, \quad (4)$$

$$Fe^{3+} + 3OH^- \rightarrow Fe(OH)_3, \quad (5)$$

$$2Fe^{3+} + 6OH^- \rightarrow \gamma\text{-}Fe_2O_3 + 3H_2O, \quad (6)$$

$$Fe^{3+} + 3OH^- \rightarrow \alpha\text{-FeOOH} + H_2O, \quad (7)$$

$$Fe^{3+} + 2H_2O \rightarrow \alpha\text{-FeOOH} + 3H^+. \quad (8)$$

3.2. Coating procedure by silanization reaction

The process of surface modification by silanization reaction is very complex. Experimental parameters such as reaction time, temperature, silane concentration and functional nature influence the reactivity of the silane molecule to the inorganic surface. The reaction between an alkoxysilane and a solid material does not involve a single mechanism, and many different intermediates are possible [14,15]. In this study, an acidic aqueous silanization procedure was used to deposit aminopropylalkoxysilane on the surface of the magnetite core. In a simplified scheme, the silanization reaction occurs in two steps. First, the organosilane is placed into an aqueous solution of an acid that acts as a catalyst. It is hydrolyzed, and a condensation reaction occurs to form a silane polymer [16]. In the hydrolysis reaction (Fig. 1),

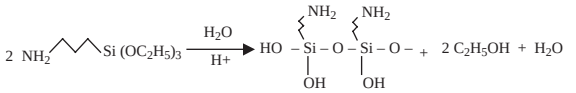

Fig. 1. Simplified reaction of hydrolysis and condensation with production of silane polymer.

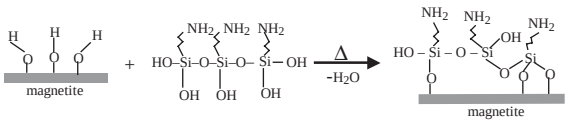

Fig. 2. Scheme of the simplified silanization reaction of (3-aminopropyl)triethoxysilane on the magnetite surface.

alkoxide groups ($-OC_2H_5$) are replaced by hydroxyl groups (OH) to form reactive silanol groups, which condense with other silanol groups to produce siloxane bonds (Si–O–Si). Alcohol (C_2H_5OH) and water are produced as by-products of condensation.

In the second step, the polymer associates with the magnetite crystallites (or surface clusters) forming a covalent bond with OH groups. Dehydration as well as adsorption of silane polymers to the metal oxide occurs. Fig. 2 shows the formation of the idealized nanoparticle of modified magnetite, i.e., APTES-magnetite [17,18], through dehydration reaction. The final product obtained from the silanization reaction in this work was dense, black and exhibited strong magnetization under a magnetic field.

3.3. X-ray diffraction

Fig. 3 shows the results of X-ray diffraction analysis for the precipitated and silanized powders. Patterns of iron oxides and oxyhydroxide products of the JCPDS database were included for comparison. Both magnetite and maghemite have a spinel structure. Their lines are close and it is difficult to distinguish them from one another by X-ray diffraction pattern. The absence of lines 110 ($d = 4.183$ Å at $2\theta = 21.22°$) and 104 ($d = 2.700$ Å at $2\theta = 33.15°$) indicates that both goethite and hematite were not formed. Peaks of $Fe(OH)_3$ ($d = 3.376$ Å at $2\theta = 26.38°$) as well as other phases of iron oxide hydroxides, γ-FeO(OH) and

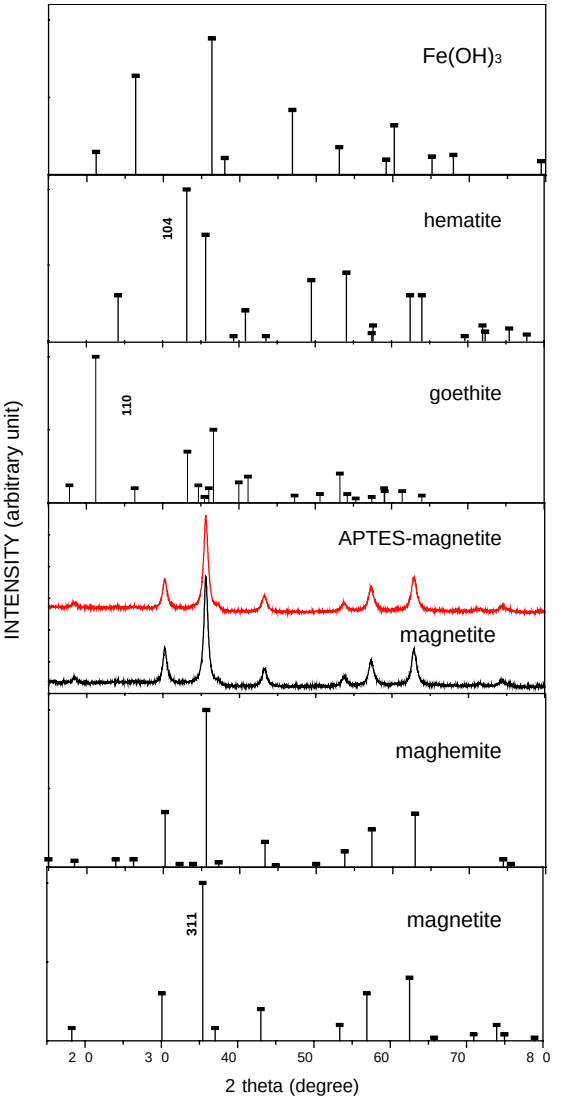

Fig. 3. X-ray powder diffraction patterns of magnetite and APTES-magnetite nanoparticles and patterns of oxides and oxyhydroxides from the JCPDS-ICDD database.

δ-FeO(OH) (not shown in Fig. 3) were not detected. As shown in Fig. 3, magnetite constituted the dominant phase in the precipitated and silanized powders, although trace amounts of maghemite may probably have formed as contaminants during the coprecipitation and silanization processes. Maghemite is brown, very different from black magnetite, but when present in trace amounts in a magnetite sample it is impossible to distinguish it by color.

The crystallite size was estimated by X-ray powder diffraction patterns from measurement of the half-height width of the strongest reflection (3 1 1) plane, using the well-known Scherrer formula [19]. Both magnetite and APTES-magnetite nanoparticles exhibited sizes equal to 12 nm. When the particles are submitted to a thermal treatment, the crystallite can grow in size and modify its physical properties. The same size was found for magnetite and APTES-magnetite crystallites, indicating that the heating on a water bath for 3 h during the silanization reaction was not sufficient to cause growth and therefore affect the physical properties of the magnetite particles.

3.4. Transmission electron micrograph and atomic force images

In order to obtain more direct information on particle size and morphology, a TEM micrograph (not shown here) of APTES-magnetite particles was done. Particles with an approximate spherical shape and an average diameter of 15 nm were observed. This may be considered as indirect evidence that the magnetite core of the APTES-magnetite particles consisted of a single magnetite crystallite with a typical diameter of 12 nm, and that the difference of 3 nm corresponds the APTES-coating.

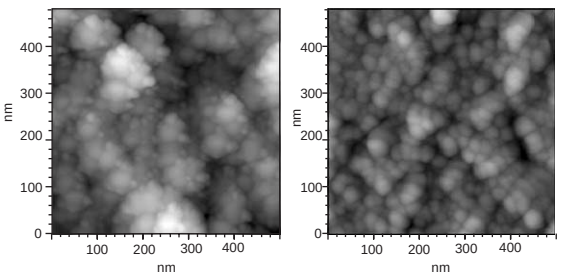

Fig. 4. MAC@ mode AFM images of films of APTES-magnetite nanoparticles obtained by depositing a microvolume of the colloidal solution the onto high-grade mica and allowing to dry at room temperature in a clean laminar flow chamber, in the absence (left) and the presence (right) of a parallel magnetic field (0.3 T).

MAC@ Mode AFM topography images of the films deposited in the absence of magnetic field (Fig. 4, left) show a peripheral distribution of nanosized particles (15–20 nm) around large clusters of variable size, reflecting the aggregation phenomena accompanying the drying process. These images complement the TEM and X-ray data, exposing the external organosilicon shell involving the magnetic nanoparticles, rather than the magnetite cores. An interesting result was obtained in the presence of a strong magnetic field (Fig. 4, right). In this case, the aggregates were much more uniform and formed round shaped clusters of about 30 nm, consistent with the association of three or four individual particles.

3.5. FTIR spectrum

In order to confirm the coating of the magnetite surface through the silanization reaction, an FTIR spectrum of the APTES-magnetite was obtained (see Fig. 5). The presence of magnetite nanoparticles can be seen by two strong absorption bands at around 632 and 585 cm^{-1}. These bands result from split of the v_1 band at 570 cm^{-1}, which corresponds to the Fe–O bond of bulk magnetite [20,21]. Furthermore, an adsorption band was observed at around 440 cm^{-1}, which corresponds to the shifting of the v_2 band of the Fe–O bond of bulk magnetite (at 375 cm^{-1}) to a higher wavenumber.

The silica network is adsorbed on the magnetite surface by Fe–O–Si bonds. This adsorption band cannot be seen in the FTIR spectrum because it appears at around 584 cm^{-1} and therefore overlaps with the Fe–O vibration of magnetite nanoparticles [22,23]. So, the adsorption of silane polymer onto the surface of magnetite particles was confirmed by bands at 1113, 1048 and 989 cm^{-1} assigned to the SiO–H and Si–O–Si groups. The absorption bands at 922 and 862 cm^{-1} revealed the presence of Si–O–H stretching and OH vibrations on the surface of magnetite. The two broad bands at 3417 and 1625 cm^{-1} can be ascribed to the N–H stretching vibration and NH_2 bending mode of free NH_2 group, respectively [17,24]. Furthermore, hydrogen-bonded silanols also absorb at around 3200 and 3470 cm^{-1} [17,25]. The presence of the anchored propyl group was confirmed by C–H stretching vibrations that appeared at 2930 and 2862 cm^{-1}.

3.6. Magnetic measurements

The APTES-magnetite nanoparticles exhibited a strong magnetization in the presence of a magnetic field. They presented a good magnetic response,

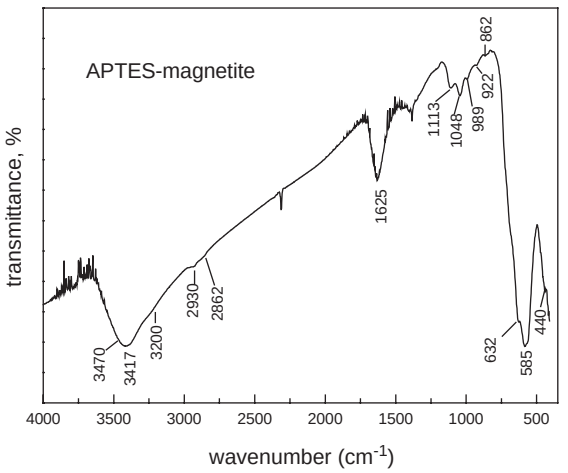

Fig. 5. FTIR spectrum of APTES-magnetite nanoparticles.

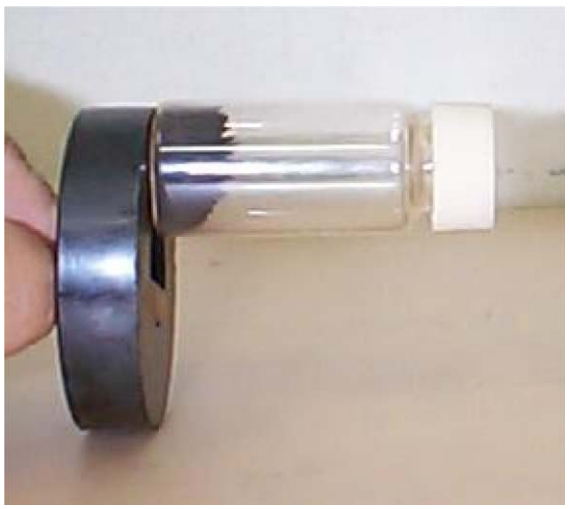

Fig. 6. APTES-magnetite nanoparticles being attracted by a magnet.

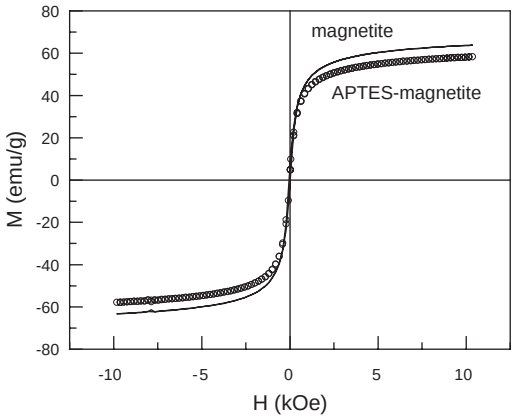

Fig. 7. Magnetization curves of magnetite and APTES-magnetite particles at 300 K.

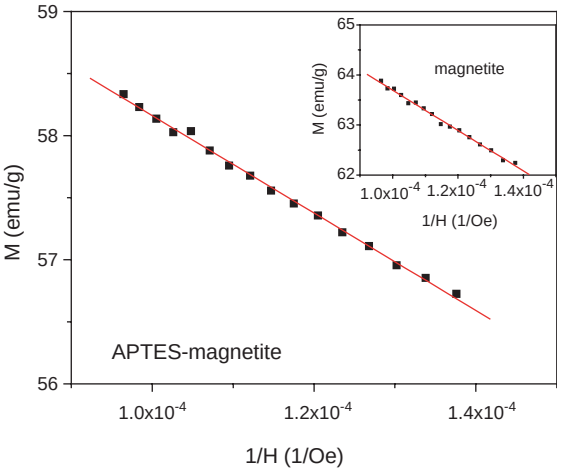

Fig. 8. Magnetization curves of magnetite and APTES-magnetite particles against the reciprocal of the applied field at 300 K.

being easily attracted by a magnet as is shown in Fig. 6.

In order to study their magnetic behavior, magnetization measurements were performed. As can be observed in Fig. 7, the magnetization curves measured for uncoated magnetite and APTES-magnetite nanoparticles showed no hysteresis and were completely reversible at 300 K. Neither coercivity nor remanence were observed. Nanoparticles exhibited typical superparamagnetic behavior [26, p. 411], a feature that is actually in accordance with what should be expected from their particle size.

Magnetic particles of size below a critical diameter exhibit superparamagnetism [26, p. 386]. An approximated value of superparamagnetic critical size, D_p, for spherical magnetite particles was calculated from the expression, $Vp \approx 25kT/K$, where k is Boltzmann constant, K = anisotropy constant ($Fe_3O_4 = 1.1 \times 10^5$ ergs cm^{-3}) [26, p. 234] and T is the absolute temperature. For 300 K, the estimated D_p was equal to 26 nm. The magnetite crystallites of the particles studied in this work have a diameter equal to 12 nm, which is below D_p (26 nm) and thus ensuring superparamagnetic behavior.

Another important parameter for practical applications of coated-nanoparticles is their magnetization. Due to the asymptotic increase of magnetization for high fields (see Fig. 7), the saturation magnetization value can be obtained from the fitting of the M vs. $1/H$ curves, extrapolating the magnetization value to $1/H = 0$ [27]. According to Fig. 8, the saturation magnetization for magnetite particles is 68 emu g^{-1}, which is lower than that of bulk magnetite (92 emu g^{-1}) [26, p. 190]. It is reported in the literature that saturation magnetization of ferrite nanoparticles sharply decreases with decreasing particle size, but the nature of this phenomenon is not clear and is still a matter of investigation. This decrease in saturation magnetization can be attributed to surface effects such as magnetically inactive layer containing spins that are not collinear with the magnetic field [28–31]. In our case, a small further reduction could be related to the contribution of a trace amount of maghemite in the total mass, which has bulk material value equal to 76 emu g^{-1} [26, p. 201]. This reduction might suggest a mixture with the maghemite phase. Discrepancies in the saturation values of magnetization reported by different groups may be explained by variations in the methods employed to synthesize magnetite, which can generate different particle sizes, magnetite surfaces and chemical compositions [32]. The saturation value obtained herein is consistent with the range of values reported in the literature [10,18]. The saturation magnetization of APTES-magnetite

particles (62 emu g^{-1}), obtained from the fitting of the M vs. $1/H$ curve shown in Fig. 8, is smaller than that of the magnetite by a factor of 9%. This can be considered an indication that the formation of the APTES coating contributes as a nonmagnetic mass to the total sample volume.

From the slope of the magnetization curve near $H = 0$, the diameter of the superparamagnetic magnetite particles can be estimated according to the expression [33]

$$D_{\mathrm{mag}} = \left(\frac{18kT(\mathrm{d}M/\mathrm{d}H)_0}{\pi\rho M_{\mathrm{s}}^2}\right)^{1/3},$$

where k is the Boltzmann constant, T is the absolute temperature, $(\mathrm{d}M/\mathrm{d}H)_0$ is the initial slope of the magnetization curve near the origin, ρ is the density of Fe_3O_4(5.24 g cm^{-3}) [26, p. 190], and M_{s} is the saturation magnetization. Taking the saturation magnetization obtained for magnetite (68 emu g^{-1}), a diameter equal to 11 nm was found, which is smaller than that obtained by TEM or X-ray diffraction. This difference could result from the extrapolated saturation magnetization value and from particle surface effects such as magnetically inert layer. The density of the magnetite, used for calculation, does not necessarily correspond to that of the true phase composition and this may have also contributed to the discrepancy.

4. Conclusions

In this work, an easy and effective method of preparation of modified magnetite nanoparticles with APTES in order to produce a superparamagnetic material with the required properties for technological applications is described. The results showed that heating of magnetite nanoparticles during the silanization reaction did not affect either particle size or their magnetic properties. The APTES-magnetite nanoparticles exhibited superparamagnetic behavior and their value of saturation magnetization was slightly lower than that of the magnetite nanoparticles; these were roughly spherical in shape and were around 15 nm in diameter. This value is very close to the size of magnetite crystallite, suggesting the formation of a continuous and very fine layer of silane on the surface of the magnetite core. The formation of pure magnetite nanoparticles was not proved, but the important result in this work is the fact that the final product exhibited strong magnetization. The APTES-magnetite nanoparticles, due to their superparamagnetic properties, high value of saturation magnetization and basic groups of amino and hydroxyl anchored on the external surface, can be used in many technological applications such as in decontamination of effluents produced by industries and nuclear power plants as well as in various bioprocesses.

Acknowledgements

This work was partially supported by the Brazilian agencies FAPESP and RENAMI/CNPq.

References

[1] J.J. Sutor, Process for preparing magnetically responsive microparticles, US Pat. 5648124, 1997.
[2] M. Koneracká, P. Kopcanský, M. Antalík, M. Timko, C.N. Ramchand, D. Lobo, R.V. Mehta, R.V. Upadhyay, J. Magn. Magn. Mater. 201 (1999) 427.
[3] A. Elaïssari, V. Bourrel, J. Magn. Magn. Mater. 225 (2001) 151.
[4] H. Gries, W. Mützel, C. Zurth, H-J. Weinmann, Magnetic particles for diagnostic purposes, US Pat. 5746999, 1998.
[5] M.H. Sousa, J.C. Rubim, P.G. Sobrinho, F.A. Tourinho, J. Magn. Magn. Mater. 225 (2001) 67.
[6] L.M. Lacava, Z.G.M. Lacava, R.B. Azevedo, S.B. Chaves, V.A.P. Garcia, O. Silva, F. Pelegrini, N. Buske, C. Gansau, M.F. Da Silva, P.C. Morais, J. Magn. Magn. Mater. 252 (2002) 367.
[7] A. Jordan, R. Scholz, P. Wust, H. Fähling, R. Felix, J. Magn. Magn. Mater. 201 (1999) 413.
[8] D.K. Kim, M. Toprak, M. Mikhailova, Y. Zhang, B. Bjelke, J. Kehr, M. Muhammed, Mater. Res. Soc. Symp. Proc. 704 (2002) W11.2.1.
[9] L. Nuñez, M.D. Kaminski, J. Magn. Magn. Mater. 194 (1999) 102.
[10] R.D. Ambashta, P.K. Wattal, S. Singh, D. Bahadur, J. Magn. Magn. Mater. 267 (2003) 335.
[11] M. Yamaura, R.L. Camilo, M.C.F.C. Felinto, J. Alloys Compd. 344 (2002) 152.
[12] M. Yamaura, R.L. Camilo, L.C. Sampaio Lima, 0302329-0/BR, Patent Pending, 2003.
[13] D.K. Kim, Y. Zhan, W. Voit, K.V. Rao, M. Muhammed, J. Magn. Magn. Mater. 225 (2001) 30.

[14] A.A. Golub, A.I. Zubenko, B.V. Zhmud, J. Colloid Interface Sci. 179 (1996) 482.
[15] G.S. Caravajal, D.E. Leyden, G.R. Quinting, G.E. Maciel, Anal. Chem. 60 (1988) 1776.
[16] C.J. Brinker, G.W. Scherer, The Physics and Chemistry of Sol-Gel Processing, Academic Press Inc., San Diego, CA, 1990.
[17] L.D. White, C.P. Tripp, J. Colloid Interface Sci. 232 (2000) 400.
[18] P.A. Heiney, K. Grüneberg, J. Fang, C. Dulcey, R. Shashidhar, Langmuir 16 (2000) 2651.
[19] B.D. Cullity, Elements of X-ray Diffraction, Addison-Wesley, Reading, MA, 1967, p. 99.
[20] R.D. Waldron, Phys. Rev. 99 (1955) 1727.
[21] Ming Ma, Yu Zhang, Wei Yu, Hao-ying Shen, Hai-qian Zhang, Ning Gu, Colloids Surf. A 212 (2003) 219.
[22] Li Guang-She, Li Li-Ping, R.L. Smith Jr., H. Inomata, J. Molec Struct. 560 (2001) 87.
[23] S. Bruni, F. Cariati, M. Casu, A. Lai, A. Musinu, G. Piccaluga, S. Solinas, NanoStructured Mater. 11 (1999) 573.
[24] Z. Xu, Q. Liu, J.A. Finch, Appl. Surf. Sci. 120 (1997) 269.
[25] S. Ramesh, I. Felner, Y. Koltypin, A. Gedanken, J. Mater. Res. 15 (2000) 944.
[26] B.D. Cullity, Introduction to Magnetic Materials, Addison-Wesley, Reading, MA, 1972.
[27] C. Liu, Z. J. Zhang, Chem. Mater. 13 (2001) 2092.
[28] D.H. Han, J.P. Wang, Y.B. Feng, H.L. Luo, J. Appl. Phys. 76 (1994) 6591.
[29] D. Lin, A.C. Nunes, C.F. Majkrzak, A.E. Berkowitz, J. Magn. Magn. Mater. 145 (1995) 343.
[30] T. Sato, T. Iijima, M. Seki, N. Inagaki, J. Magn. Magn. Mater. 65 (1987) 252.
[31] R.H. Kodama, J. Magn. Magn. Mater. 200 (1999) 359.
[32] M. Grigorova, H.J. Blythe, V. Blaskov, V. Rusanov, V. Petkov, V. Masheva, D. Nihtianova, Ll.M. Martinez, J.S. Muñoz, M. Mikhov, J. Magn. Magn. Mater. 183 (1998) 163.
[33] N.A.D. Burke, H.D.H. Stöver, F.P. Dawson, Chem. Mater. 14 (2002) 4752.